A Comparison Study of Nonlinear State Observer Design: Application to an Intensified Heat-Exchanger/Reactor

Xue Han, Zetao Li, Michel Cabassud, Boutaib Dahhou

A Comparison Study of Nonlinear State Observer Design: Application to an Intensified Heat-Exchanger/Reactor*

Xue Han [1] Zetao Li [2] Michel Cabassud [3] Boutaib Dahhou [4]

Abstract— **In this paper, five classical nonlinear state observers: extended Luenberger observer (ELO), extended Kalman filter (EKF), high-gain observer (HGO), sliding mode observer (SMO) and adaptive observer (AO), are applied to an intensified chemical heat exchanger/reactor (HEX reactor). In order to choose a suitable observer to develop a new fault diagnosis algorithm for this high nonlinear system, the behaviors of these observers are compared. The maximum overshoot and the settling time, which are the key features of the dynamic of the output estimation error system, are used as the criteria to compare the performances of the observers. Both cases with and without measurement noise are considered. It is concluded that the AO presents the fastest convergence speed and the minimum oscillation for the application to the HEX reactor. And the information provided by the AO will be further used for its fault diagnosis.**

I. INTRODUCTION

With the increment of the complexity of industrial systems, it is difficult to supervise all the internal states during production. However, these process states are critical features to indicate whether the system functions normally or not. Especially for the reactors which are extensively operated in chemical, food, and pharmaceutical industries, unexpected deviation in temperature or concentration of the reactant will result in serious consequence. Therefore, it proposes a high demand for detailed information on system states. The state observers, which use the structure of the real system and a minimum set of measurements, can provide the estimation of the actual states of the system in real time.

After the original work by Luenberger [1], a variety of methods for state estimation of nonlinear systems have been proposed in the literature [2]–[4]. In most cases, an adequate mathematical model of the plant is necessary. Extended Luenberger observer (ELO) [5] and extended Kalman filter (EKF) [6] are both derived from linear cases based on first-order linearization. Unlike the ELO, the EKF can perform a state estimation which is robust concerning measurement noise. However, the dynamic uncertainties, as well as the measurement uncertainties, pose great challenges in the process of state estimation. To overcome them, high-performance robust observers have been widely considered. Based on the work of [7], a high-gain observer (HGO) is developed not only for single-output system but also multi-output system [8]. The sliding-mode observer (SMO) [9], which is based on the sliding-mode principle, can precisely estimate the internal states by generating a sliding motion on the sliding surface [10], [11]. When unknown parameters exist in real system, an adaptive observer (AO) is proposed, where both system states and unknown parameters can be estimated at the same time. Early results on adaptive observer were presented in [12], and further developed by [13], [14]. Since all the observers have the information of the system states, they are helpful for the following operations, like controller design [11], [15], fault diagnosis [14], [17] and fault tolerant control [16], [18].

Unlike the traditional batch reactor, the intensified HEX reactor is a sort of plug-flow chemical reactor which combines heat exchanger and chemical reactor in one minimized module [19]. Due to its complexity and high nonlinearity, it is a challenging task to construct an observer to supervise all the internal states during the process of production. And that also makes it difficult to diagnose and identify the potential faults. Our main goal is choosing a suitable nonlinear observer to estimate all the system states and provide sufficient information to the further fault diagnosis, identification (FDI) and fault tolerant control (FTC).

In this paper, five classical nonlinear observers are applied to the HEX reactor system in an open loop. The performances of the observers are compared and presented in the cases with and without measurement noise. Since the characteristics of different observers vary a lot due to the change of the observer gain. It is difficult to compare the behaviors of different observers. In this work, the maximum overshoot and the settling time of the estimation error system, which separately indicates the stability and the convergence speed, are considered as the criteria for this comparison. The observer gain is chosen to satisfy one request and the other criterion is compared. The observer which estimates the states with the minimum overshoot and the shortest settling time is the suitable choice for further FDI and FTC use.

The paper is organized as follows. Section II gives an introduction to the classical observer design techniques. Then, an intensified HEX reactor, which acts as the target system, is presented. In section IV, the considered observers are applied

[1]Xue Han is with LAAS-CNRS, Université de Toulouse, CNRS, INSA, UPS, 31400 Toulouse, France xue.han@laas.fr

[2]Zetao Li is with Electrical Engineering College,Guizhou University, 550025 Guiyang, China (corresponding author) gzgylzt@163.com

[2]Michel Cabassud is with Laboratoire de Génie Chimique, Université de Toulouse, CNRS/INPT/UPS, 31432 Toulouse, France michel.cabassud@ensiacet.fr

[2]Boutaib Dahhau is with LAAS-CNRS, Université de Toulouse, CNRS, INSA, UPS, 31400 Toulouse, France boutaib.dahhou@laas.fr

to this HEX reactor, and the comparison results between different observers are performed under two cases: with and without measurement noise. Finally, after comparing the behaviors of the state observers, concluding remarks are proposed in the last section.

II. NONLINEAR STATE ESTIMATION TECHNIQUES

Considering the nonlinear system in a state space form:

$$\begin{aligned} \dot{x} &= f(x,u) \\ y &= h(x) \end{aligned} \tag{1}$$

where x represents the state vector, u is the input vector, and y is the measured output vector.

The general structure of a state observer, which consists of a copy of the original model and a correction term, is written as follows:

$$\begin{aligned} \dot{\hat{x}} &= f(\hat{x},u) + K(y-\hat{y}) \\ \hat{y} &= h(\hat{x}) \end{aligned} \tag{2}$$

where $\hat{x}$ and $\hat{y}$ are the estimations of the state vector x and output vector y. The gain of the observer, denoted by K, determines the convergence properties of the state estimator.

Define the estimation error:

$$e = x - \hat{x} \tag{3}$$

Then the error dynamic is derived:

$$\dot{e} = f(x,u) - f(\hat{x},u) - K(h(x) - h(\hat{x})) \tag{4}$$

Thus, the observer design problem is reformulated as choosing a suitable gain K such that the estimation error dynamic (4) is asymptotically stable. Five classical nonlinear observers used in this paper are presented in the following.

A. Extended Luenberger Observer

As is shown in the name, 'extended' indicates that it is an extension of the original linear version to nonlinear systems. By linearizing the nonlinear system at an operation point, the ELO is constructed by the same method as used to design a Luenberger observer.

Considering the nonlinear system (1), the extended Luenberger observer is constructed in the same form as (2). After the linearization of (4), we obtain:

$$\dot{e} = (F - KH)e \tag{5}$$

where F and H are calculated by:

$$F = \left[\frac{\partial f(x,u)}{\partial x}\right]_{x=\hat{x}}, \quad H = \left[\frac{\partial h(x)}{\partial x}\right]_{x=\hat{x}} \tag{6}$$

The observer gain K is chosen by satisfying the eigenvalues of $(F-KH)$ have strictly negative real parts. The estimation accuracy of the ELO relays on how well the linearized model represents the nonlinear dynamics. For this reason, the ELO is more easily applied to less complex nonlinear systems.

B. Extended Kalman Filter

The extended Kalman filter is an extension of Kalman filter, which is considered as a stochastic problem as well as a deterministic optimization problem [3].

Considering the time-varying nonlinear system with process noise and measurement noise:

$$\begin{aligned} \dot{x} &= f(x,u) + \eta, \quad \eta \sim \mathcal{N}(0,Q) \\ y &= h(x) + \varsigma, \quad \varsigma \sim \mathcal{N}(0,R) \end{aligned} \tag{7}$$

where η and ς represent the process noise and the measurement noise, which are random variables with Gaussian distribution. Their corresponding variances are Q and R, respectively.

Then, the EKF is constructed in the same form of (2). The observer gain K equals to:

$$K = SH^T R^{-1} \tag{8}$$

where S is the solution of:

$$\dot{S} = FS + SF^T + Q - SH^T R^{-1} HS \tag{9}$$

F and H are both calculated by the linearization (6).

As mentioned in the ELO design, the EKF is also limited to a small space for the reason that the model linearization has a strict limitation of the operation point. Besides, its robust can not be guaranteed if there are modeling errors.

C. High Gain Observer

Considering an input affine system:

$$\begin{aligned} \dot{x} &= f(x) + g(x)u \\ y &= h(x) \end{aligned} \tag{10}$$

Using diffeomorphism $\phi = [h \quad L_f h \quad \dots \quad L_f^{n-1} h]^T$, where $L_f h$ represents the Lie derivative of h along f, this input affine system (10) can be transformed to a canonical form (11):

$$\begin{aligned} \dot{x} &= \begin{bmatrix} \dot{x}_1 \\ \dot{x}_2 \\ \vdots \\ \dot{x}_{n-1} \\ \dot{x}_n \end{bmatrix} = \begin{bmatrix} x_2 \\ x_3 \\ \vdots \\ x_n \\ \varphi(x) \end{bmatrix} + \begin{bmatrix} g_1(x_1) \\ g_2(x_1,x_2) \\ \vdots \\ g_{n-1}(x_1,\dots,x_{n-1}) \\ g_n(x_1,\dots,x_n) \end{bmatrix} u \\ &= Ax + Gu \\ y &= x_1 = Cx \end{aligned} \tag{11}$$

where $A = \begin{bmatrix} 0 & I_{n-1} \\ 0 & 0 \end{bmatrix}$, $C = \begin{bmatrix} 1 & 0 & \dots & 0 \end{bmatrix}$. $\varphi(x)$ is a nonlinear function. I represents the identity matrix, n is the dimension of the real system.

Assume that each component $g_i (i = 1,2,\dots,n)$ and $\varphi(x)$ are global Lipschitz, Gauthier [7] has proposed a high-gain observer:

$$\dot{\hat{x}} = f(\hat{x}) + g(\hat{x})u - S_\infty^{-1} C^T (C\hat{x} - y) \tag{12}$$

where S_∞ is the unique solution of the Lyapunov algebraic equation:

$$\theta S_\infty + A^T S_\infty + S_\infty A - C^T C = 0 \tag{13}$$

θ is chosen large enough to control the speed of convergence, and that is the reason why it is called the high-gain observer.

Besides, the high-gain observer provides an exponential convergence of the estimation error. However, the transformation is challenging to calculate sometimes, and a very high gain may cause the peaking phenomenon.

D. Sliding Mode Observer

Based on the theory of sliding mode, a sliding mode observer [9] has been proposed. As an inherent property, SMO is insensitive to parameter uncertainties or external disturbance signals, which makes it a proper choice for state estimation.

For the nonlinear system (11), a sliding mode observer is designed as follows:

$$\dot{\hat{x}} = A\hat{x} + Gu - K_l(C\hat{x} - y) - K_n sign(C\hat{x} - y) \tag{14}$$

where the K_l is chosen such that $(A - K_l C)$ is stable, and K_n is a key factor to determine the bandwidth on the patch. Increasing the bandwidth may potentially reduce the sensitivity to measurement noise.

From its initial value, the convergence of the estimation error e is divided into two steps. The first step is the sliding surface design. When the system is barred to the designed sliding surface, the expected performance is achieved. In the next step, a variable structure control law is designed, then the system trajectory is driven to the sliding surface and maintains a sliding mode after transition time. As long as the sliding surface is reached, the estimation becomes insensitive to the disturbances. And then, the estimation error is forced by the sliding mode observer to converge to zero, which means that the estimated states converge to the actual states.

E. Adaptive Observer

The adaptive observer is also a well-known robust observer which can estimate the system states under the parameter uncertainties and modeling errors. Early works on adaptive observers for linear systems can be tracked back to the 70s. And the design for the nonlinear cases started from the early 90s. Then, it is widely used in actuator, sensor and process fault diagnosis.

As proposed in [14], when the fault occurs in the lth actuator of the system (10), we have $u_l^f = u_l + f_{al} = \theta_{al}$, where f_{al} is a constant and u_l^f is the actual output of the lth actuator when it is faulty, while u_l is the expected output when it is healthy. The corresponding faulty model is:

$$\begin{aligned} \dot{x} &= f(x) + \sum_{j \neq l} g_j(x) u_j + g_l(x)\theta_{al}, \quad j = 1, 2, \ldots, m \\ y &= h(x) \end{aligned} \tag{15}$$

where $g(x) = [g_1(x), g_2(x), \ldots, g_m(x)]$, m is the number of the actuator..

Then, the adaptive observer for the faulty system (15) is:

$$\begin{aligned} \dot{\hat{x}} &= f(x) + \sum_{j \neq l} g_j(x) u_j + g_l(x)\hat{\theta}_{al} + K_y(\hat{x} - x) \\ \dot{\hat{\theta}}_{al} &= -2\gamma(\hat{x} - x)^T K_\theta g_l(x) \end{aligned} \tag{16}$$

where K_y is a Hurwitz matrix that it can be choose freely with a goal to increase as much as possible the dynamic of the observer. γ is a design constant and K_θ is a positive definite matrix that satifies:

$$K_y^T K_\theta + K_\theta K_y = -Q \tag{17}$$

where Q is a positive definite matrix that can be chosen freely.

After the transition time, the AO will give the accurate estimation of the real system states and the faulty actuator output u_l^f if the gain is chosen suitably. But a suitable gain matrix that can increase the dynamic of the observer is difficult to choose sometimes.

III. CASE STUDY: AN INTENSIFIED HEX REACTOR

The intensified HEX reactor considered in this paper is a module that combines heat exchanger and chemical reactor. Its effictiveness has been investigated in [19].

A. Physical Structure of the intensified HEX Reactor

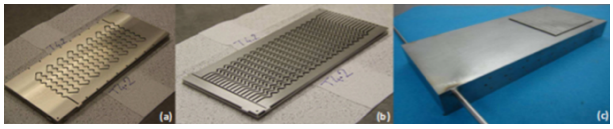

Fig. 1: Physical structure of the HEX reactor [19]: (a)Process channel; (b)utility channel; (c)the physical HEX/Reactor

The physical structure of the HEX reactor is shown in Fig.1. It is composed of three process plates sandwiched between four utility plates, which are all engraved with 2 mm square cross-section channels. The plate wall is the steel between channels, and it acts as the heat exchange media. The process flow, which consists of varible reactants, is injected into the process channel, where the chemical reaction is taken place. A utility fluid is injected into the utility plat with a flow rate F_u to heat the process flow or take away the heat generated by the reaction. A multi cell-based model is proposed in [20]. And the effectiveness of this model has been verified by the comparison between simulation results and experimental data.

B. Mathematical Modelling

For simplicity, only the heat exchange part is considered in this paper. Water with different temperatures ($T_{p,in}$, $T_{u,in}$) is injected into process channel and utility channel respectively. Define the state vector as $x = [T_p \quad T_u \quad T_w]^T$, the control input $u = F_u$, the measurable variable $y = T_p$. According to

the energy balance equation, the mathematical model of the HEX reactor is:

$$\begin{aligned}
\dot{T}_p &= \frac{F_p}{V_p}(T_{p,in} - T_p) + \frac{h_p A_p}{\rho_p V_p C_{p,p}}(T_w - T_p) \\
\dot{T}_u &= \frac{F_u}{V_u}(T_{u,in} - T_u) + \frac{h_u A_u}{\rho_u V_u C_{p,u}}(T_w - T_u) \\
\dot{T}_w &= \frac{h_p A_p}{\rho_w V_w C_{p,w}}(T_p - T_w) + \frac{h_u A_u}{\rho_w V_w C_{p,w}}(T_u - T_w)
\end{aligned} \tag{18}$$

where the subscript p, u and w represent the process fluid, utility fluid and plate wall, the subscript *in* represents the inlet fluid. $h(\mathrm{W}\cdot\mathrm{m}^2\cdot\mathrm{K}^{-1})$ is the heat transfer coefficient. $\rho(\mathrm{kg}\cdot\mathrm{m}^{-3})$, $V(\mathrm{m}^3)$, $A(\mathrm{m}^2)$ and $C_p(\mathrm{J}\cdot\mathrm{kg}^{-1}\cdot\mathrm{K}^{-1})$ are density, volume, heat exchange area and specific heat of material respectively. $F(\mathrm{m}^3\cdot\mathrm{s}^{-1})$ is the volume flow rate. $T(\mathrm{K})$ is the temperature.

The model above is just for one cell, which may cause slightly differences in the dynamic behavior of the real reactor. However, the observer application and the final state estimation performance will not be affected.

IV. SIMULATION RESULTS AND DISCUSSION

To illustrate the effectiveness of the state estimation, the observers presented are applied to the HEX reactor presented in section III. Table I gives the nominal values of the operating conditions used in the simulation. And the related experimental data can be found in [19].

TABLE I: Physical Data of The Pilot

Constant	Value	Units
V_p	2.68×10^{-5}	m^3
ρ_p, ρ_u	10^3	$\mathrm{kg}\cdot\mathrm{m}^{-3}$
$C_{p,p}, C_{p,u}$	4.186×10^3	$\mathrm{J}\cdot\mathrm{kg}^{-1}\cdot\mathrm{K}^{-1}$
A_p	2.68×10^{-2}	m^2
V_u	1.141×10^{-4}	m^3
A_u	4.564×10^{-1}	m^2
V_w	1.355×10^{-3}	m^3
ρ_w	8×10^3	$\mathrm{kg}\cdot\mathrm{m}^{-3}$
$C_{p,w}$	5×10^2	$\mathrm{J}\cdot\mathrm{kg}^{-1}\cdot\mathrm{K}^{-1}$

In this study, different initial values are given to the real system and the observer to investigate the behavior of state estimation. And all the observers are provided with the same initial values in order to compare their performance of convergence. The initial temperatures (°C) of the HEX reactor are $x(0) = [T_p(0) \quad T_u(0) \quad T_w(0)]^T = [17.6 \quad 39.7 \quad 25]^T$, the initial temperatures (°C) provided to observers are $\hat{x}(0) = \left[\hat{T}_p(0) \quad \hat{T}_u(0) \quad \hat{T}_w(0)\right]^T = [20 \quad 42 \quad 25]^T$. The temperatures of the inlet fluids ($T_{p,in}$, $T_{u,in}$) for the reactor and observers are the same as their corresponding initial values. The mass flow rate $(\mathrm{kg}\cdot\mathrm{s}^{-1})$ for process plates and utility plates are 14 $\mathrm{kg}\cdot\mathrm{s}^{-1}$ and 113 $\mathrm{kg}\cdot\mathrm{s}^{-1}$. Since the temperature of the process fluid (T_p) can be measured directly while the temperature of utility fluid (T_u) is immeasurable (it can be obtained in simulation), the output estimation error $e_{T_u} = \hat{T}_u - T_u$ is the one that we considered for the comparison. Generally, the estimation error will converge to zero after a period of time. However, for a unique observer, different gain values will result in the various dynamics of the estimation error system. So, it is not easy to compare the performances of five classical observers. In this paper, the maximum overshot $|\delta_m|$ and the settling time t_s are considered as the main features to represent the dynamic of the estimation error system. The maximum overshoot is defined as the maximum peak value of the output error curve measured from zero. And the settling time is defined as the time required for the output error curve to reach and stay within a range around zero. To start, one of the main features of the estimation error system is fixed at a set point, and then, it can be reached by choosing suitable gains for each observer. Finally, the other can be compared to investigate the performance of the observers. The smaller the value $|\delta_m|$ is, the more gentle oscillation the system has. The shorter settling time it takes, the faster convergence speed it has. In this paper, the maximum overshoot is fixed as $\delta_m = -20\% \times e_{T_u}(0)$, where $e_{T_u}(0) = \hat{T}_u(0) - T_u(0)$, and the range is set as $\pm 2\% \times e_{T_u}(0)$. Moreover, the performances of the state estimation with and without measurement noise are both taken into consideration.

A. Case 1:Noise free

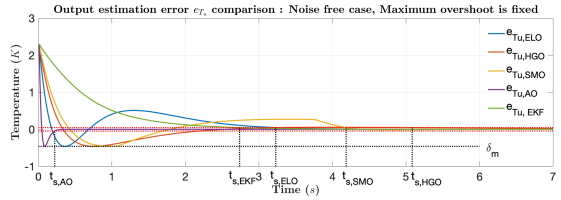

(a) Output estimation error of ELO, HGO, SMO, AO and EKF

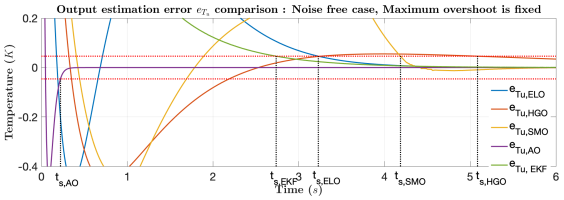

(b) Zoom in

Fig. 2: Noise free case: output estimation error comparison (Situation 1: Maximum overshoot is fixed).

In this case, the system is well known and without measurement noise. In order to compare the performances of the presented observers, two situations are considered. Firstly, the maximum overshoot of the output estimation error system is fixed. Then, the settling time, which indicates the convergence speed, has been compared to understand the convergence behavior of each observer. Secondly, the settling time has been fixed. Then the stability of each output estimation error system has been presented by comparing the maximum overshoots generated by the considered observers. The comparison results are shown in Fig.2 and Fig.3. It should pay attention to the EKF, both of the variances of process noise and that of measurement noise are the key parameters to determine its estimation behavior. In this paper,

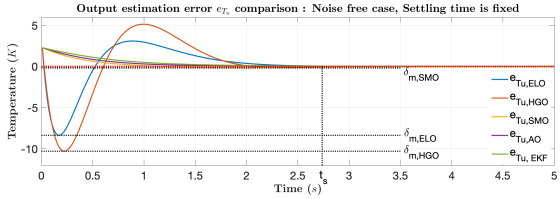

(a) Output estimation error of ELO, HGO, SMO, AO and EKF

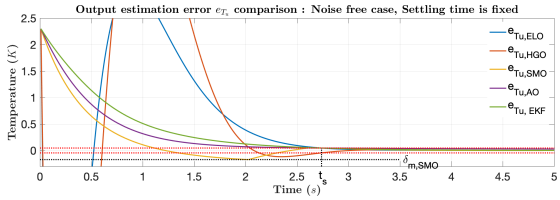

(b) Zoom in

Fig. 3: Noise free case: output estimation error comparison (Situation 2: Settling time is fixed).

they are set at quite small values (1.0×10^{-3} and 1.0×10^{-4} respectively) to investigate its performance under the noise free case.

According to Fig.2, the maximum overshoot of each observer is fixed at $\delta_m = -20\% \times e_{T_u}(0) = 0.46$, which is represented by the black dotted line in the figure. The settling time for each observer varies from $0.22s$ to $5.09s$. The red dotted lines represent the envelopes to indicate the settling time. It is obvious that the adaptive observer has the shortest settling time, which means it has the fastest convergence speed, while the high gain observer takes the longest time to estimate the real states. In Fig.3, the settling time is fixed at $2.74s$, which equals to the time that the EKF used to estimate the states where its parameters can not be adjusted in this case. The value of the maximum overshoot $|\delta_m|$ of each observer performs differently. The estimation error generated by EKF and AO both converges to zero without oscillation. Among the rest three observers, HGO provides the maximum overshoot while SMO offers the minimum overshoot. The ELO has an overshoot a little smaller than that of HGO.

TABLE II: Comparison Between Observers: Noise Free Case

Type of observers	Number of parameter to be adjusted	Situation 1: Maximum overshoot fixed		Situation 2: Settling time fixed	
		Settling time $t_s(s)$	Maximum overshoot $\lvert\delta_m\rvert(K)$	Settling time $t_s(s)$	Maximum overshoot $\lvert\delta_m\rvert(K)$
ELO	1	3.23	0.46	2.74	8.35
HGO	2	5.09			10.28
SMO	2	4.19			0.17
AO	3	0.22			0
EKF	2				0

The exact values of settling time and maximum overshoot under these two situations are presented in Table II. The observer gain vector K is considered as one parameter to be adjusted, the dimension of the gain vector equals to the dimension of the system state vector. In conclusion, the AO has better performance under both situations in noise free case.

B. Case 2: With measurement noise

In the second case, the measurement noise is considered, a white Gaussian noise with a variance of 0.01 has been added to the output of the HEX reactor. After that, the same situations have been considered to compare the performance of each observer: maximum overshoot is fixed and settling time is fixed. For the EKF, the variance of process noise is chosen the small value (1.0×10^{-3}) as that in noise free case, while the variance of measurement noise is set as 0.01 to cooperate with the measurement noise case. The behaviors of the observers, which correspond to different situations are presented in Fig.4 and Fig.5.

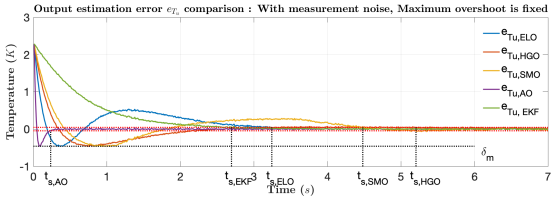

(a) Output estimation error of ELO, HGO, SMO, AO and EKF

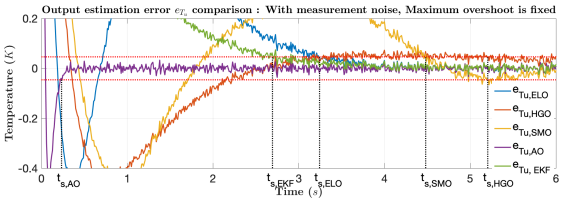

(b) Zoom in

Fig. 4: With measurement noise: output estimation error comparison (Situation 1: Maximum overshoot is fixed).

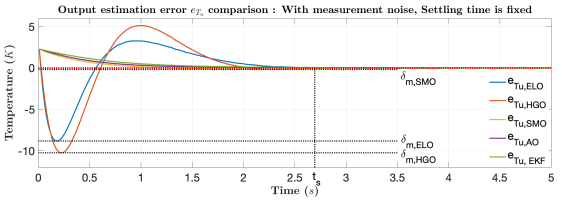

(a) Output estimation error of ELO, HGO, SMO, AO and EKF

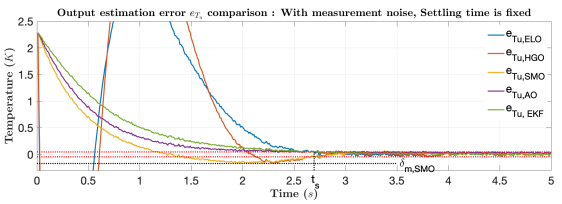

(b) Zoom in

Fig. 5: With measurement noise: output estimation error comparison (Situation 2: Settling time is fixed).

When the measurement noise is considered, the observers present similar results as in noise free case. Under situation one where the maximum overshoot $|\delta_m|$ is fixed, AO still has the shortest convergence time of $0.23s$. In contrast, the longest time for state estimation is still generated by HGO

(5.20s). According to Fig.5, the settling time t_s is settled at 2.70s, which equals to the time that the EKF takes for state estimation where its gains are fixed. Both the estimation errors of EKF and AO are still vibrationless, while the HGO gives the greatest oscillation. The ELO provides an overshoot smaller than HGO, but much bigger than that of SMO. The exact values of the overshoot and the settling time under each situation are given in Table III. The AO still performs better than other observers when the measurement noise is considered.

TABLE III: Comparison Between Observers: With Measurement Noise

Type of observers	Number of parameter to be adjusted	Situation 1: Maximum overshoot fixed		Situation 2: Settling time fixed	
		Settling time $t_s(s)$	Maximum overshoot $\lvert\delta_m\rvert(K)$	Settling time $t_s(s)$	Maximum overshoot $\lvert\delta_m\rvert(K)$
ELO	1	3.24	0.46	2.70	8.81
HGO	2	5.21			10.24
SMO	2	4.48			0.17
AO	3	0.24			0
EKF	2				0

V. CONCLUSION

In this paper, five types of nonlinear observers are applied to a high nonlinear HEX reactor system: two classical extended observers (ELO, EKF) based on global linearization, and three kinds of robust observers (HGO, SMO, AO). In order to choose an observer that can offer the shortest converge time and minimum oscillation for further FDI use, the performances of these observers are compared and presented here. The maximum overshoot indicates the stability of the observer, and the settling time reveals the convergence speed. These two features are considered as the criteria to evaluate the dynamic of estimation error system. Under the first situation, suitable gains are chosen to make the estimation error system reached the fixed maximum overshoot to compare the settling time of each observer. After that, the settling time is fixed, and the maximum overshoot corresponding to every observer are analyzed. Finally, the comparison results are provided separately according to the existence of measurement noise. In both cases, AO has the minimum oscillation and the fastest convergence speed, while HGO presents the most significant oscillation and the slowest convergence speed. In addition, the EKF performs good which is vibrationless and has a relatively fast convergence speed. The ELO is limited by its quite big oscillation when the settling time is fixed, and the SMO takes a relatively long time to estimate the real states when the overshoot is fixed.

In conclusion, the adaptive observer is a suitable choice for state estimation of the HEX reactor. And it will be used to develop a new algorithm for the fault diagnosis and identification of the intensified HEX reactor. Moreover, some operations like fault tolerant control can also be applied to avoid accidental situations and provide a safe production environment.

REFERENCES

[1] D. Luenberger, Observers for multivariable systems, IEEE Transactions on Automatic Control, vol. 11(2), 1966, pp. 190-197.

[2] E. A. Misawa, and J. K. Hedrick, Nonlinear observers—a state-of-the-art survey, Journal of dynamic systems, measurement, and control, vol. 111(3), 1989, pp. 344-352.

[3] D. Dochain, State and parameter estimation in chemical and biochemical processes: a tutorial, Journal of process control, vol. 13(8), 2003, pp. 801-818.

[4] G. Besançon, Nonlinear observers and applications, Berlin: springer, 2007.

[5] T. Meurer, On the extended Luenberger-type observer for semilinear distributed-parameter systems, IEEE Transactions on Automatic Control, vol. 58(7), 2013, pp. 1732-1743.

[6] T. Moore, and D. Stouch, A generalized extended kalman filter implementation for the robot operating system, Intelligent autonomous systems 13, Springer, 2016.

[7] J. P. Gauthier, H. Hammouri, and S. Othman, A simple observer for nonlinear systems applications to bioreactors, IEEE Transactions on automatic control, vol. 37(6), 1992, pp. 875-880.

[8] H. Hammouri, G. Bornard, and K. Busawon, High gain observer for structured multi-output nonlinear systems, IEEE Transactions on automatic control, vol. 55(4), 2010, pp. 987-992.

[9] S. K. Spurgeon, Sliding mode observers: a survey, International Journal of Systems Science, vol. 39(8), 2008, pp. 751-764.

[10] V. Utkin, J. Guldner, and J. Shi. Sliding mode control in electro-mechanical systems, CRC press, 2017.

[11] K. Kumari, A. Chalanga, and B. Bandyopadhyay, Implementation of super-twisting control on higher order perturbed integrator system using higher order sliding mode observer, IFAC-PapersOnLine, vol. 49(18), 2016, pp. 873-878.

[12] G. Besançon. Remarks on nonlinear adaptive observer design, Systems & control letters, vol. 41(4), 2000, pp. 271-280.

[13] T. A. Najafabadi, F. R. Salmasi, and P. Jabehdar-Maralani, Detection and isolation of speed-, DC-link voltage-, and current-sensor faults based on an adaptive observer in induction-motor drives, IEEE Transactions on Industrial Electronics, vol. 58(5), 2010, pp. 1662-1672.

[14] D. Fragkoulis, G. Roux, and B. Dahhou, Detection, isolation and identification of multiple actuator and sensor faults in nonlinear dynamic systems: Application to a waste water treatment process, Applied Mathematical Modelling, vol. 35(1), 2011, pp. 522-543.

[15] M. Ghanes, M. Trabelsi, H. Abu-Rub, and L. Ben-Brahim, Robust adaptive observer-based model predictive control for multilevel flying capacitors inverter, IEEE transactions on industrial electronics, vol. 63(12), 2016, pp. 7876-7886.

[16] Z. Li, N. Kabbaj, B. Dahhou, and J. Aguilar-Martin, Fault-tolerant control for nonlinear dynamic systems, Proc. IFC Symposium on power plants and power systems control, 2003.

[17] M. Zhang, B. Dahhou, M. Cabassud, and Z. Li, Faults Isolation and Identification of Heat-Exchanger/Reactor with Parameter Uncertainties, DX@ Safeprocess, 2015, pp. 253-260.

[18] Z. Makhataeva, B. Sarsembayev, and D. D. Ton, Fault-Tolerant Control of IPMSMs Based on an Modified Sliding Mode Observer, 2019 International Conference on System Science and Engineering (ICSSE), IEEE, 2019, pp. 526-530.

[19] F. Theron, Z. Anxionnaz-Minvielle, M. Cabassud, C. Gourdon, and P. Tochon, Characterization of the performances of an innovative heat-exchanger/reactor, Chemical Engineering and Processing: Process Intensification, vol. 82, 2014, pp. 30-41.

[20] M. He, Z. Li, X. Han, M. Cabassud, and B. Dahhou, Development of a Numerical Model for a Compact Intensified Heat-Exchanger/Reactor, Processes, vol. 7(7), 2019, pp. 454.